Subscription Agency
Exploring and Distributing Knowledge Globally

Innovations in Emerging Technologies and its Applications
Volume 1 Issue 1

Investigation of Inverse Population in Graphene Using Boltzmann Transfer Function Method

S.Sadegh Najafi*
Department of Chemical Engineering, Faculty of Engineering, Islamic Azad University-Chabahar Branch, Chabahar, Iran, IR 9971777548
Corresponding Author
Email Id: sadeq.najafi.88@gmail.com

ABSTRACT

In this research, first graphene and its structure are introduced, and then we have studied its properties. Finally, the inverse population in graphene is estimated according to the Boltzmann transfer function. In the next section, we first examine the Hamiltonian graphene, and then write the transition rate for the carrier phonon and carrier photons. Finally, using the equilibrium equations written based on the Boltzmann transfer equation and the relation to the total number of carriers, we obtain the chemical potential of the holes and the electrons. The assumption for this calculation is that graphene is placed on the SiC substrate in the form of interwoven growth and its initial chemical potential is non-zero. The polarization of incoming light to graphene is in the x direction. Now, if we consider the interaction of light beam and carriers in graphene and the interaction of phonon carriers as a disorder, we calculate the Hamiltonian. The Columbus modulus was used to obtain the interaction of the carrier and the incident light.

Keywords: *Graphene, Inverted population, Light polarization.*

INTRODUCTION

The issue of carbon and the structures produced from it is a fascinating and wide-ranging issue. First fluorine and then carbon nanotubes were made in 1991 and after twelve years of graphene in 2003 by a group led by Gaim and Novoslov. Wallace had long ago predicted the properties of graphene using a tight binding model [1]. In 2003, what Wallace had predicted more than fifty years ago came true and showed the same properties. In order to define two-dimensional structures, we consider a high limit on the number of atoms that, if higher, are no longer considered two-dimensional. For a semiconductor, there must be between 10 and 100 atomic layers on top of each other [2]. Attempts to produce graphene as a two-dimensional material using conventional methods were not sufficient because the system still tends to go three-dimensional due to thermal fluctuations, and its two-dimensionality is unstable. But the solution is to contact graphene with 3D systems to make it stable. To do this, graphene can be created on or between two three-dimensional materials [2]. The band structure of single-layer graphite, or graphene, was first studied by Wallace in 1947. In that paper, the band structure and properties of graphene under equilibrium conditions are fully investigated. But the behavior of carriers in graphene in non-equilibrium conditions is different from equilibrium conditions. The results of one of the first examinations of carriers using femto second tail show that, firstly, graphite, due to its anisotropy, prevents the carrier from propagating perpendicular to each graphite plate (graphene). This means that if we give energy to graphite, this energy is propagated in two dimensions within it. This makes graphite very suitable for studying the electron plasma dynamics and two-dimensional holes. Secondly, its

metalloid properties have both semiconductor and metallic properties. That is, graphene can produce electrons and holes by excitation, which is a semiconductor-like behavior, and on the other hand is similar to metals due to the lack of a gap.

The structure of the graphene honeycomb is shown in Figure 1. If we look at each cell, it is as if two triangles have penetrated each other so that, for example, atom B of one triangle is right in the middle of the side of the other triangle made of atom A. Each atom has one s orbital and three p orbitals. The s orbitals and two of the ps in the graphene plate are strongly clamped by the covalent force and do not participate in the conduction, but the remaining p orbitals are perpendicular to the graphene plate and are under odd rotation and hybridize from the capacitance band to the conduction band.

The length of the carbon-carbon bond in graphene is aC-C = 1.42 A °. The structure of the graphene honeycomb can be thought of as a Bravais lattice with two atoms per single cell, shown in Figure 1 as A and B. Thus, two π electrons per unit cell participate in the electronic properties of graphene. The band structure of graphene is plotted in Figure 2 and it is clear that the capacitance and conduction bands are connected without gaps. The best description for the electronic structure of graphene is to use the approximation of the nearest neighbor in the tight binding method [1]. Graphene has two atoms in its single cell, which leads to two cone points in each Brillouin region. Near these points the energy is linearly dependent on the wave vector That is, a relation in the form $E = v_f \hbar \vee K \vee$Where v_f is the Fermi velocity which is 1/300 the speed of light. We denote the density of states in graphene by $g_{2d} = \frac{2E}{\pi \hbar^2 v_0^2}$.

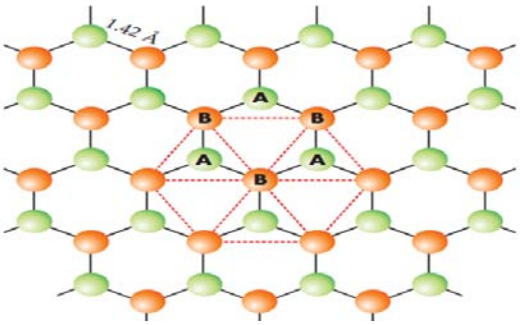

Fig. 1. Graphene Honeycomb Structure with Two Atoms per Single Cell

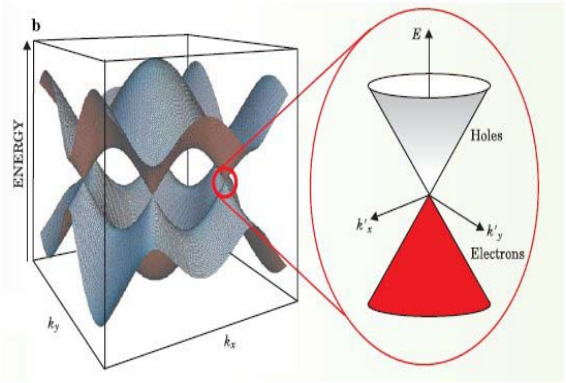

Fig. 2. Graphene Band Structure

INDIVIDUAL PROPERTIES OF GRAPHEME

1. Quantum v effect: This effect, like most other quantum phenomena, requires a low temperature to observe, which is usually lower than the boiling point of liquid helium [4]. Attempts to increase in observing temperature of the Hall Effect have been unsuccessful. For example, one solution is to use semiconductors with low effective mass but they have not been able to raise the observation temperature of the Hall Effect above 30 K. In graphene, the quantum Hall Effect can be observed even at room temperature, due to the behavior of the particles in graphene, which behave like relativistic particles without mass [4]. The semi-intiger quantum Hall Effect has also been observed in graphene [5].

2. Klein paradox: This paradox refers to the free penetration of relativistic particles into a wide potential barrier. In the case of non-relativistic particles, the probability of tunneling has an exponential relationship with the height of the barrier, but in relativistic particles, such as electrons in graphene, the probability of crossing the potential barrier is one [6]. The electrons in graphene are called Dirac electrons [11].

Investigation of Inverse Population in Graphene by Boltzmann Transfer Function Method

In this section, we first examine the grapheme Hamiltonian. Then we write the transition rate for the phonon-carrier and photon-carrier modes. Finally, using the balance equations based on the Boltzmann transfer equation and the relation to the total number of carriers, we obtain the chemical potential of the holes and the electrons. The assumption for this calculation is that graphene is placed on the SiC substrate in the form of interwoven growth and its initial chemical potential is non-zero. The polarization of incoming light to graphene is in the x direction. Now, if we consider the interaction of light beam and carriers in graphene and the carrier-phonon interaction as a disorder, Hamiltonian is in equation (1):

$$H = H_0 + H_{Perturbation} \quad (1)$$

That $H_0$is the grapheme Hamiltonisn in the non-perturbation state which is (2):

$$H_0 = v_f \sigma.P \quad (2)$$

Which σ is a Pauli matrices and is defined as (3):

$$\sigma_z = \begin{pmatrix} 1 & 0 \\ 0 & -1 \end{pmatrix}, \ \sigma_y = \begin{pmatrix} 0 & -i \\ i & 0 \end{pmatrix}, \ \sigma_x = \begin{pmatrix} 0 & 1 \\ 1 & 0 \end{pmatrix} \quad (3)$$

The graphene Hamiltonian is as follows:

$$H_0 = v_f \begin{pmatrix} 0 & P_x - iP_y \\ P_x + iP_y & 0 \end{pmatrix} \quad (4)$$

We write the perturbation Hamiltonian as (5):

$$H_{Perturbation} = H_{C-phot} + H_{C-phon} \quad (5)$$

Where H_{C-phot} is related to the interaction of the carrier and the incident light and H_{C-phon} is related to the interaction of the phonon and the carrier. To obtain the interaction of the carrier and the incident light, we use the Coulomb gauge as $P \to P + eA(t)$ in which we place the absolute value of the electron instead of e. So for Hamiltonian we have the interaction of light and graphene (6):

$$H_{C-phot} = eA_x(t)V_f \begin{pmatrix} 0 & 1 \\ 1 & 0 \end{pmatrix} \qquad (6)$$

The polarization of the incident light is in the x direction, which is applied in Equation (6). Where $A_x(t) = \frac{F_0 sin(\omega t)}{\omega}$where F_0 is the electric field intensity and ω is the frequency of the light emitted. In the following, we will study the carrier of the phonon Hamiltonian. Here we only consider optical phonons because during the period when we have an inverse population, the temperature is very high, at which temperature optical phonons are present in the system [8]. To calculate the optical phonon Hamiltonian, we first introduce the following function [9]:

$$u(r) = \sum_{q,\zeta} \sqrt{\frac{\hbar}{2NM\omega_0}} \left(b_{q\zeta} + b^{\dagger}_{-q\zeta}\right) e_{\zeta}(q) e^{iq.r} \qquad (7)$$

N is the number of unit cells and M is the mass of each carbon atom and $\omega_0$of the optical phonon frequency at point Γ is 0.196 ev. $q = (q_x, q_y)$ The wave vector and ζ represent the type of wave, transverse t or longitudinal l, and finally $b^{\dagger}_{-q\zeta}$and $b_{q\zeta}$represent the operators of creation and annihilation. We define wave vectors as follows:

$$q_y = qSin\varphi(q) \qquad ,q_x = qCos\varphi(q) \qquad (8)$$

Where q = | q | . $e_{\zeta}(q)$ for longitudinal and transverse modes are as follows:

$$e_t(q) = i\left(-sin\varphi(q), cos\varphi(q)\right) \qquad ,, e_l(q) = i\left(cos\varphi(q), sin\varphi(q)\right) \qquad (9)$$

The interaction of the electron and the optical phonon at point K is as follows:

$$H^{K'}_{C-phon} = -\sqrt{2}\frac{\beta\gamma}{b^2}\sigma \quad \times u(r) \qquad ,, H^{K}_{C-phon} = -\sqrt{2}\frac{\beta\gamma}{b^2}\sigma \times u(r) \qquad (10)$$

Where $b = \frac{a}{\sqrt{3}}$ is the bond length in equilibrium conditions and $\gamma = \hbar v_f$ and the parameter β are represented as follows:

$$\beta = \frac{-d(ln\gamma_0)}{d(lnb)} 2 \qquad (11)$$

Finally, the Hamiltonian of electron-phonon interaction is as follows:

$$H_{C-phon} = -\sqrt{\frac{\hbar}{2NM\omega_0}} \sqrt{2}\frac{\beta\gamma}{b^2} \sum_{q,\zeta} \left(b_{q\zeta} + b^{\dagger}_{-q\zeta}\right) V_{\zeta}(q) e^{iq.r} \qquad (12)$$

Where $V_{\zeta}(q)$ for longitudinal and transverse wave is represented as follows:

(13)

$$V_i^K(q) = \begin{pmatrix} 0 & -exp\left(-i\varphi_q(q)\right) \\ exp\left(i\varphi_q(q)\right) & 0 \end{pmatrix}$$

$$V_t^K(q) = \begin{pmatrix} 0 & iexp\left(-i\varphi_q(q)\right) \\ iexp\left(i\varphi_q(q)\right) & 0 \end{pmatrix}$$

For the point K' is $V_\zeta^{K'}(q) = V_\zeta^K(-q)$ where φ_q is the angle between q and the x-axis.

To calculate the probability of transition, we must use the Fermi's golden rule, which we will explain at first, then we will get the results of probability of transition per unit time or the same rate of transition for perturbed Hamilton's. The Fermi's golden rule is for calculating the transition rate in which we use time-dependent perturbation. To use this Hamiltonian rule, we consider the system as $H=H_0+H_{Perturbation}$ and the eigen value based on the special expansion of the ground eigenvector which has a time factor as $\psi(t) > \sum_n c_n(t) \vee \varphi_n(t) > exp\left(\frac{-iE_n t}{\hbar}\right)$ will expand.

Now we have three assumptions to calculate the transition rate:

1) The system is in the initial state in |i> state and the probability of its presence in any other state is zero.
2) The perturbation is weak and is applied for a short time so that it does not change the states of the system and special conditions before the system perturbation can be used to describe it.
3) Direct shifting is done from |i> to |f> and the probability of any other shifting is zero.
   The important point in the golden rule is the states of the system that can no longer be used if they are changed during the perturbation. If we consider the perturbation in the system to be time-dependent, like when a laser pulse strikes an object and the frequency of this pulse is resonant, $\omega\omega_{fi}$, after mathematical operations, we reach the following relation for the transfer rate: (14)

$$W = \frac{2\pi}{\hbar} w_{fi}^2 \delta\left(E_f - E_i\right)$$

In which $w_{fi} = \psi_f |H_{Perturbation}| \psi_i >$, Introduce the total transition rate for the system as $W_{\lambda,\lambda'}(k,k') = \sum_v W_{\lambda,\lambda'}^v (k,k')$ where λ = 1 for conduction band and $\lambda = -1$ for valence band. v

Represents a variety of dispersion processes. If we show the state of the electronic system with $\frac{1}{\sqrt{2}}\begin{pmatrix} 1 \\ \lambda exp\,(i\varphi) \end{pmatrix} exp\,(ik.r)$ for the carrier-photon track we have: (15)

$$W_{\lambda,\lambda'}^{C-Phot\pm}(k,k') = \frac{2\pi}{\hbar}\frac{1}{2}\left(\frac{eF_0\gamma}{\hbar\omega}\right)^2 \frac{1+\lambda\lambda' cos(2\varphi)}{2} \delta_{k,k'} \delta\left[E_\lambda(k) - E_{\lambda'}(k') \pm \hbar\omega\right]$$

Where the positive sign refers to absorption and the negative sign refers to photon production, and φ refers to the angle k and the x-axis. The details of the calculation are such that if we place the Hamiltonian between the initial state and the final state of the system, we have a $exp(i(k-k').r)$statement that if on both sides of the equation, the integral $\frac{1}{2\pi}\int_0^{2\pi} dr$multiply to the left becomes one and right to the definition of the Kronecker delta, which means:

$$\Delta_{x,y} = \frac{1}{2\pi}\int_0^{2\pi} exp(i(x-y)z)dz$$

$\delta_{k',k}$and the Dirac delta sentence, depending on whether the system is irradiated by photons with energy $\hbar\omega$ or we choose the absorption of negative and positive answers, respectively and the sentence $\frac{1+\lambda\lambda' cos(2\varphi)}{2}$ is obtained by placing the matrix in the perturbation between the initial and final state.

Instead of $sin^2(\omega t)$ we put the average. For carrier-phonon we have: (16)

$$W_{\lambda,\lambda'}^{C-Phon,\pm}(k,k') = \frac{2\pi}{\hbar}\begin{pmatrix} N_q \\ N_q+1 \end{pmatrix} u_{\lambda,\lambda'}^{C-Phon}(q,\theta) \vee {}^2\delta_{k',k+q}\delta\left[E_\lambda(k) - E_{\lambda'}(k') \pm \hbar\omega_q\right]$$

Where$N_q = \frac{1}{exp\left(\frac{\hbar\omega_q}{k_B T}\right)-1}$ is the phonon occupation number, where $N_q + 1$ refers to the production and N_q refers to the phonon absorption, and θ is the angle between k and k ' And u for l and t are defined respectively as follows:

$$u_{\lambda,\lambda'}^{l}(q,k) \vee \frac{g\gamma}{\sqrt{2}}\sqrt{1-\lambda\lambda' cos(\varphi-\varphi'-2\varphi_q)} \qquad (17)$$

$$u_{\lambda,\lambda'}^{t}(q,k) \vee \frac{g\gamma}{\sqrt{2}}\sqrt{1+\lambda\lambda' cos(\varphi-\varphi'-2\varphi_q)}$$

The details of the calculation of $W_{\lambda,\lambda'}^{C-Phon,\pm}(k,k')$ after placing a perturbation Hamiltonian are between $\psi_{tot} > \vee \psi_{elec} > \otimes \vee \psi_{phon} >$which $\psi_{phon} >$ is related to phononic mode:

$$exp(i(q+k-k').r) < \psi'_{phon} | b + b^\dagger | \psi_{phon} >$$

The sentence $exp(i(q+k-k').r)$ is related to the representation of the general state, which has an exp(ik.r) of the electronic state and an exp(iq.r) of the phononic state. exp(ik'.r) means the final state of the electronic system. If we multiply the integral equation $\frac{1}{2\pi}\int_0^{2\pi} dr$on both sides, according to what has been said, we have $\delta_{k',k+q}$ and the answer $\psi'_{phon}|b+b^\dagger|\psi_{phon}>$ is that, either the final state has a higher energy than the initial one (due to phonon absorption) or less (due to phonon radiation) depending on $\delta[E_\lambda(k) - E_{\lambda'}(k') \pm \hbar\omega]$ is defined and $\begin{pmatrix} N_q \\ N_q+1 \end{pmatrix}$is created. Sentence $|u_{\lambda,\lambda'}^{C-Phon}(q,\theta)|$It is also

obtained by placing $V_\zeta(q)$ between $\frac{1}{\sqrt{2}}\begin{pmatrix}1\\ \lambda exp(i\varphi)\end{pmatrix}$ (which for the final state φ becomes φ') and its size is multiplied by two. In the next step, we use the equilibrium equation [12-10], which is based on the Boltzmann equation: (18)

$$\frac{\partial f_\lambda(k)}{\partial t} = g_s g_v \sum_{\lambda',k',v}\left[F^v_{\lambda'\lambda}(k',k) - F^v_{\lambda\lambda'}(k,k')\right]$$

Where $g_s = 2$refers to the spin degeneracy and $g_v = 2$refers to the Vady degeneracy, $F^v_{\lambda'\lambda}(k',k)$ is introduced as follows: (19)

$$F^v_{\lambda'\lambda}(k',k) = f_{\lambda'}(k')[1 - f_\lambda(k)]W^v_{\lambda'\lambda}(k',k)$$

Where $f_\lambda(x) = \frac{1}{1+exp\left(\frac{x-\mu_\lambda}{k_B T}\right)}$is a Fermi-Dirac distribution function where $\mu_\lambda$is the chemical potential. To calculate the equilibrium relation, we use the mass balance equation [13], which is obtained by multiplying $g_s g_v \sum_k$ in relation (18). Now we calculate that if λ = 1 we have a function for the distribution of electrons and for λ = -1 we have a function for the distribution of holes, for which the relation $n_e = g_s g_v \sum_k f_{+(k)}$and for the holes.

We have the relation $n_h = g_s g_v \sum_k$ [11].

To calculate the electron, the relation is known, but for the hole, we multiply equation (18) by negative, then add $-f_{-(k)}$to a sum (due to the conversion of the relation to n_h).

The reason it is permissible is that we add a fixed number in front of the derivative that has no effect on the derivative, and finally we get the following relation: (20)

$$\frac{\partial n_e}{\partial t} = \frac{\partial n_h}{\partial t} = \frac{n_h}{\tau_{-+}\ v - \frac{n_e}{\tau_{+-}\ v}}$$

Where $\frac{1}{\tau^v_{\lambda'\lambda}} = \frac{16}{n_{\lambda'}}\sum_v F^v_{\lambda'\lambda'}$ as can be seen from Equation (20), a change in the population of the conduction band is equal to a change in the population of the capacitance band. It also states that only the transition between the bands can change the population of the bands. Now using Equation (20) and assuming a stable equilibrium condition $\frac{\partial n_e}{\partial t} = \frac{\partial n_h}{\partial t} = 0$ (which, as mentioned earlier, this stable equilibrium is not more than a few femto-second) we reach the following relation:

$$F_{-+}\ co_{+}+F_{-+}\ cp_{-}=F_{+-}\ co_{-}+F_{+-}\ cp_{+} \qquad (21)$$

The sentences are as follows:

$$F_{-+}\ co_{+}=\frac{se^2F_0^2}{s\hbar^2\omega}f_{-}\left(\frac{-\hbar\omega}{2}\right) \qquad (22)$$

$$F_{+-}{}^{co_-} = \frac{\pi e^2 F_0^2}{\varepsilon \hbar^2 \omega} f_{+}\left(\frac{\hbar\omega}{2}\right) \quad (23)$$

$$F_{+-}{}^{cp_-} = \frac{\pi g^2 (N_0+1)}{\pi h \gamma^2} \int_0^{\hbar\omega_0} dx x(\hbar\omega_0 - x) f_{+(x)} \quad (24)$$

$$F_{-+}{}^{cp_+} = \frac{\pi g^2 N_0}{\pi h \gamma^2} \int_0^{\hbar\omega_0} dx x(\hbar\omega_0 - x) f_{-(-x)} \quad (25)$$

Equation (22) refers to the absorption of a photon and its transfer from the capacitance band to the conduction, and Equation (23) refers to the emission of a photon during the transfer from the conduction band to the capacitance. Equations (24) and (25) shows with the propagation are emission and absorption of phonon during inter-band transfer, respectively. In Equation (19), statements like $F_{-+}{}^{co_-}$ or $F_{+-}{}^{co_+}$ are zero. This is because the former represents the emission of a photon during the transfer of an electron to the conduction band, and the latter indicates the absorption of a photon by the electron in the conduction band, which is zero due to the lowlifespan of the electron and the need for high energy for this process. The process of calculating the expressions is such that, as we have studied before, we want to arrive at a mass equilibrium relation. To calculate (22) considering the Cronecker delta operations that cause k = k ':

$$\frac{\partial n_g}{\partial t} = \frac{2\pi}{\hbar} \frac{1}{2} \left(\frac{eF_0\gamma}{\hbar\omega}\right)^2 \int_0^{+\infty} dE f_{-(k)} \quad (26)$$

Above, we applied the properties what we mentioned in the Dirac Delta. To apply the Dirac delta means to place $\frac{\hbar\omega}{2}$ in the distribution functions and E in the density of the states (note that the delta was originally $\delta[-E(k) - E(k) + \hbar\omega]$ and instead We put $E_{-1}(k) = -E(k)$ and we put $E_1(k) = E(k)$ then we applied the mentioned property for factorization). Because of the electron distribution of the case, the density of the states $\frac{\hbar\omega}{2}$ put in E and in the function $f_{+(k)}$ but in $f_{-(k)}$ we have to put $\frac{-\hbar\omega}{2}$ because it is related to the holes. For the angle we set π / 3.

Here it is mathematically clear why $\lambda = \lambda'$ a value of zero has because the Dirac delta becomes $\delta[\pm\hbar\omega]$ which is zero. The calculation (23) is the same. To calculate (24) again, as mentioned, we apply the Cronecker Delta [14] and considering that:

$$n(E)D(E)dE = \sum \delta(E_F - E_i)dE \quad (27)$$

$D(E)$ is the density of states: (28)

$$\frac{\partial n_g}{\partial t} = \frac{2\pi}{\hbar}\left(N_q + 1\right)\left|u_{\lambda\lambda'}^{C-Phon}(q,\theta)\right|^2 \int_0^{\hbar\omega} dE D(E) f_{+(k')}$$

Note that above the density of states is based on the conduction band and based on $E_+(k')$. So to apply the Dirac delta, we write it according to what has been, based on the density of states, and we have:

$$E_+(k'-q) = E_-(k') + \hbar\omega_q = -E(k') + \hbar\omega_q \quad (29)$$

So the density of states is obtained as $\frac{2(-E(k')+\hbar\omega_q)}{\pi\gamma^2}$ (we write this expression instead of Dirac delta). We also put the expression in the distribution function $f_{-(k'-q)}$. In addition, we consider that the distribution is related to the hole $f(E(k')-\hbar\omega_q)$. If we also write the density of states, we have an $E(k')$ and we put x in the whole expression instead of $E(k')$ and the relation (24) is obtained. We do the same for relation (25). Now consider a graphene sample whose conductive carriers are in the absence of an electron field. After applying the field, the electrons are excited from the conduction band, in which case the number of electrons becomes:

$$n_e = n_0 + \Delta n_e \qquad (30)$$

$\Delta n_e = n_h, n_0$is the amount of initial pollution. To calculate the chemical potential of electrons μ_e and holes μ_h, by solving equations (21) and (30) simultaneously, unknowns can be found. To perform the calculations, it should be noted that sentences (24) and (25) are for the propagation emission or absorption of a phonon by an electron, and the transmission between bands is considered in this case. The energy of an optical phonon in graphene is about 0.196 ev. Now, if we study the initial equations, it becomes clear that almost the excitation of an electron by the absorption of a phonon is possible only if the energy of the electron is less than 0.1 ev in the valence band (This energy is possible from $\frac{0.196}{2}$ in the valence band to $\frac{0.196}{2}$ in the conduction band), which we have drawn in Figure 3 for better expression. Another point that can be seen in Figure 3 is that if the electron wants to be transferred to the conduction band, according to the Pauli Exclusion Principle, the final state should not be full and the transfer to the electron should not be allowed. This means that the chemical potential should not be more than about 0.1 ev in the conduction band. If we consider more than this, sentences (24) and (25) should be deleted because if the chemical potential is greater than 0.1 ev, the sentences lose their effectiveness. In the calculations according to what we observed in the second part for the excitation temperature, the temperature is much higher than 300 K, so we set higher values for the temperature and examined the results at 2000K, 1200K and 750K.

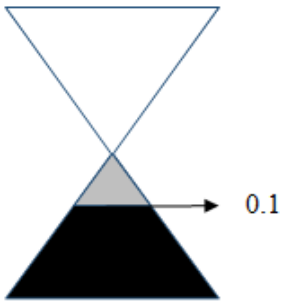

Fig. 3. The graphene band structure is plotted and only the gray area can be excited by optical phonons, and less so for the black area we have no excitation by the phonon. If it is produced by transferring an electron from a conduction band to a phonon, the electron must be transferred to the gray area. Note that we considered the phonon energy to be approximately 0.2 ev.

As shown in Figure 4, we have plotted the normalized conductivity to σ_0 in this diagram. The first normal conductivity starts from a value of one for each energy, which means that in the absence of graphene radiation conductivity, is the same as σ_0. But then, as the electrical conductivity increases, it decreases. That is, it moves towards negative values and reaches the maximum values mentioned in the figure for each conductivity. As we said before, this means that there is light amplification in graphene. Conductivity, which if we compare here with the values obtained in the previous section, we find that there was an absolute value of the maximum negative conductivity of a larger value. In addition, at each intensity emitted, we observed that the temperature is approximately higher than 1500 K, but here, as the temperature rises (and approaches the values expected in the laboratory), the conductivity decreases. The following are the reasons for this behavior. As we have seen, the values obtained behaved logically. That is, with increasing field and more arousal, we reached negative conduction. But the data obtained should be numerically larger. So we have to choose mechanisms to improve the numbers obtained. These mechanisms can include software, the type of equation writing, or physical discussions.

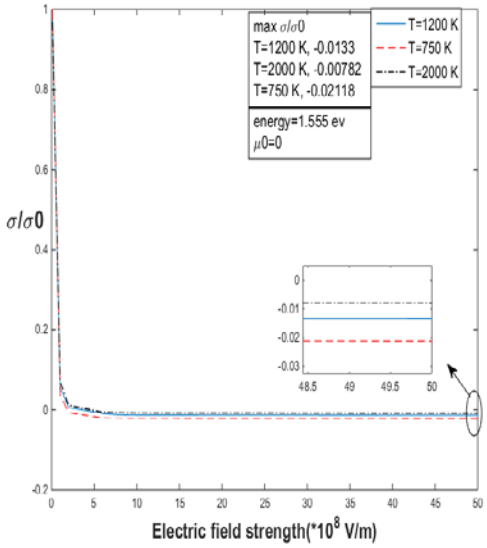

Fig. 4. Conductivity changes normalized to σ_0 for intensity changes for three different temperatures.

CONCLUSION

In order to solve the equations, due to the complexity of the obtained sentence, we chose the numerical solution. To do this, we used the CDOS (Conjugate Direction with Orthogonal Shift) Mathematical optimization method, which is available as a package for Maple software. In this type of solution, first the answer of each function is obtained for the given interval, then any point that was common between them is considered as the answer of the device. For example, if the first equation of a polynomial is equal to zero and the second is equal to zero, we firstly specify an interval. Then, in this interval, the program tests for which numbers each of the functions is zeroed in the given interval (which, of course, does not have to be zero, if the limit set for the answer is 8-10, each of the answer numbers To this extent or less is considered as the answer of the function). In the end, each of the functions

was solved in the same way. The answer of the device is the common answers of all these functions. In the solution process, after simultaneously solving equations (21) and (30), we calculated the chemical potential values of the electrons and holes. If we study the values obtained from the chemical potential solution, it can be seen that if the chemical potential is 0.02 ev greater than the state (for example) 2000 k, the graph obtained for the initial chemical potential is zero and the temperature is mentioned and the energy is 1.65 ev as Figure 5 is obtained. Of course, the energy of 1.65 ev is not special, and if we add the same level of energy to each answer in this range, one or half percent, we will see this change. As can be seen, this small difference in calculation causes a large change in conductivity and is almost very close to the expected values. This process in solving equations and calculations is due to the rounding of numbers that takes place. Therefore, techniques that reduce this process should be used as much as possible But due to the solution that is done in the CDOS method, we did not find a way to prevent rounding. The fact that the conductivity decreases with increasing temperature can also be explained in the same way. That is, because the temperature is increased by a power from 750 K to 2000 K, and the temperature decreases the coefficient of the equation, this condition enhances the rounding, and deviate the answer from the expected values. Another possibility that can be controlled by a better answer is to simplify the equation and find small sentences and remove them from the equation. Similar sentences can be combined. Extending some of them to polynomials can also be a very useful method along with the previous solutions. We did not do this because there are complex sentences to solve. The reason is that we can get the answer to the principle of the calculated equation. Of course, it should be noted that in the previous section, when we expanded the sentences, we could completely write the equation in terms of polynomials, and the method was simpler and there was very little possibility of error.

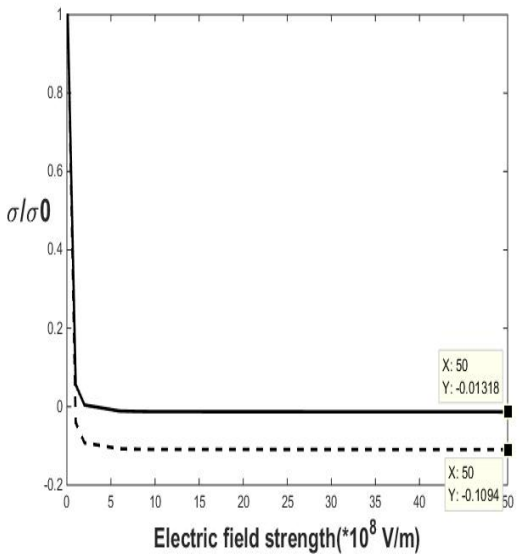

Figure 5. Conductivity change diagram in terms of field strength change for energy 1.65 ev where the line represents the actual values calculated and the dashed line the values for manually adding 0.02 ev to the answer. This graph shows the sensitivity of the answer to the small digits obtained from the equation. Is. Note that dashed line values are not real values.

Another reason that causes a difference in the calculated results and the expected results is not considering the temperature for each applied intensity. As we saw in the previous section, we had different temperatures to reach different n_{ex}. As it turns out, the higher the intensity, the higher the n_{ex}. As we have seen, the temperature behavior with n_{ex} also increases with increasing this factor. This shows that we must apply a specific temperature for each intensity. In the calculations we applied the same temperature in terms of maximum intensity, which is the same for all intensities. There are two ways to solve this problem. The first is to completely solve the Boltzmann equation, which allows the temperature to be calculated accurately. The second and better way is to use the Green function and consider a quantum field and an self-energy and complete quantum problem solving. In Figure 6 below, we plot the conduction changes for different intensities. But this time the chemical potential has a non-zero value of 0.08 ev, but why are the results not different from zero? If we do not consider the effect of rounding, this is also the expectation physically here. Because the chemical potential of 0.08 ev is slightly less than the quantum optical phonon energy. The only effect of chemical potential can be effective when we have exactly 0.098 ev (ev = 0.196 / ev =) in the conduction band that fills the states and there is no space for electron transfer. So with this amount of chemical potential, the final answer should not change.

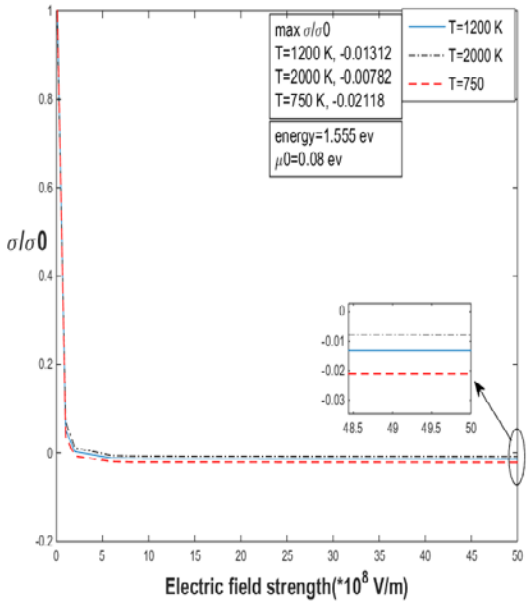

Fig. 6. Conductivity changes normalized to σ_0 for different intensities for three different temperatures at a chemical potential of 0.08 ev.

REFERENCES

1) P.R. Wallace, The Band Theory of Graphite, Physical Review, 71 (1947) 622-634.
2) Mehdi Darbandi; “Proposing New Intelligent System for Suggesting Better Service Providers in Cloud Computing based on Kalman Filtering”; Published by HCTL International Journal of Technology Innovations and Research, (ISSN: 2321-1814), Vol. 24, Issue 1, PP. 1-9, Mar. 2017, DOI: 10.5281/Zenodo.1034475.

3) Mehdi Darbandi; "Proposing New Intelligence Algorithm for Suggesting Better Services to Cloud Users based on Kalman Filtering"; Published by Journal of Computer Sciences and Applications (ISSN: 2328-7268), Vol. 5, Issue 1, 2017; PP. 11-16; DOI: 10.12691/JCSA-5-1-2; USA.
4) Mehdi Darbandi; "Kalman Filtering for Estimation and Prediction Servers with Lower Traffic Loads for Transferring High-Level Processes in Cloud Computing"; Published by HCTL International Journal of Technology Innovations and Research, (ISSN: 2321-1814), Vol. 23, Issue 1, pp. 10-20, Feb. 2017, DOI: 10.5281/Zenodo.345288.
5) S. Haghgoo, M. Hajiali, A. Khabir, "Prediction and Estimation of Next Demands of Cloud Users based on their Comments in CRM and Previous usages", International IEEE Conference on Communication, Computing & Internet of Things; Feb. 2018, Chennai. DOI: 10.1109/IC3IoT.2018.8668119.
6) C. Rostamzadeh, F. Canavero, F. Kashefi "Automotive AM-Band Radiated Emission Mitigation Techniques, a Practical Approach", International IEEE Symposium on Electromagnetic Compatibility; Aug. 2012, Pittsburgh, USA. DOI:10.1109/ISEMC.2012.6351791.
7) Mehdi Darbandi, M. Abedi; "involving Kalman filter technique for increasing the reliability and efficiency of cloud computing", International WORLD COMPETITION 2012; Los Vegas, USA.
8) P. Shahbazi; "New Novel idea for Cloud Computing: How can we use Kalman filter in security of Cloud Computing", International IEEE Conf. AICT.; Oct. 2012, Georgia, Tbilisi. DOI:10.1109/ICAICT.2012.6398466.
9) F. Kashefi "Perusal about influences of Cloud Computing on the processes of these days and presenting new ideas about its security", International IEEE Conf. AICT., Dec. 2011, Baku, Azerbaijan. DOI:10.1109/ICAICT.2011.6111007.
10) H. Sahin, O. Leenaerts, S.K. Singh, F.M. Peeters, Graphane, Wiley Interdisciplinary Reviews: Computational Molecular Science, 5 (2015) 255-272.
11) K.S. Novoselov, Z. Jiang, Y. Zhang, S.V. Morozov, H.L. Stormer, U. Zeitler, J.C. Maan, G.S. Boebinger, P. Kim, A.K. Geim, Room-Temperature Quantum Hall Effect in Graphene, Science, 315 (2007) 1379-1379.
12) Y. Zhang, Y.-W. Tan, H.L. Stormer, P. Kim, Experimental observation of the quantum Hall effect and Berry's phase in graphene, Nature, 438 (2005) 201-204.
13) M.I. Katsnelson, K.S. Novoselov, A.K. Geim, Chiral tunnelling and the Klein paradox in graphene, Nat Phys, 2 (2006) 620-625.
14) J.R. Lima, F. Moraes, Indirect band gap in graphene from modulation of the Fermi velocity, Solid State Communications, 201 (2015) 82-87.
15) E. Hwang, S.D. Sarma, Acoustic phonon scattering limited carrier mobility in 2D extrinsic graphene, arXiv preprint arXiv:0711.0754, (2007).
16) T. Ando, Magnetic oscillation of optical phonon in graphene, Journal of the Physical Society of Japan, 76 (2007) 024712-024718.
17) W. Xu, F. Peeters, J. Devreese, Diffusion-to-streaming transition in a two-dimensional electron system in a polar semiconductor, Physical Review B, 43 (1991) 14134-14141.
18) H. Dong, W. Xu, F. Peeters, High-field transport properties of graphene, Journal of Applied Physics, 110 (2011) 063704-063709.
19) H. Dong, W. Xu, Z. Zeng, T. Lu, F. Peeters, Quantum and transport conductivities in monolayer graphene, Physical Review B, 77 (2008) 235402-235410.
20) W. Xu, H. Dong, L. Li, J. Yao, P. Vasilopoulos, F. Peeters, Optoelectronic properties of graphene in the presence of optical phonon scattering, Physical Review B, 82 (2010) 125304-125312.
21) D. Snoke, The quantum Boltzmann equation in semiconductor physics, Annalen der Physik, 523 (2011) 87-100.

22) S. Moiseev, Universal derivative-free optimization method with quadratic convergence, arXiv preprint arXiv:1102.1347, (2011).
23) A. Ramtin, O. Sharafi, "Tasks Mapping in the Network on a Chip Using an Improved Optimization Algorithm", Published by International Journal of Pervasive Computing and Communications, Vol. 16, Issue 2, PP. 165-182, 2020. https://doi.org/10.1108/IJPCC-07-2019-0053.
24) S. Norozpour, "Proposing New Method for Clustering and Optimizing Energy Consumption in WSN"; Published by International Journal of Talent Development & Excellence (ISSN: 1869-0459), Vol. 12, No. 3S, PP. 2631-2643, 2020.
25) S. Seyedi, N. J. Navimipour; "Designing an efficient fault tolerance D-latch based on quantum-dot cellular automata nanotechnology"; Published by Optik Journal, (ISSN: 0030-4026), Vol. 185, PP. 827-837, May 2019. DOI:10.1016/j.ijleo.2019.03.029
26) Bashirov, A. E., & Norozpour, S. (2018). On an alternative view to complex calculus. *Mathematical Methods in the Applied Sciences*, *41*(17), 7313-7324.
27) BASHIROV, A. E., & Norozpour, S. (2017). On complex multiplicative integration. *TWMS Journal of Applied and Engineering Mathematics*, *7*(1), 82-93.
28) ERGÜN, C., & Norozpour, S. (2019). Farsi document image recognition system using word layout signature. *Turkish Journal of Electrical Engineering & Computer Sciences*, *27*(2), 1477-1488.